Molecular orbital ordering in titania and the associated semiconducting behavior

Joseph Park,[1] Kyung-Chul Ok,[1] Byung Du Ahn,[2] Je Hun Lee,[2] Jae-Woo Park,[2] Kwun-Bum Chung,[3,a)] and Jin-Seong Park[1,b)]
[1]*Department of Materials Science and Engineering, Dankook University, Mt. 29, Anseo-Dong, Cheonan 330-714, Republic of Korea*
[2]*Samsung Electronics, Giheung-Gu, Yongin-Si, Gyeonggi-Do 446-711, Republic of Korea*
[3]*Department of Physics, Dankook University, Mt. 29, Anseo-Dong, Cheonan 330-714, Republic of Korea*

(Received 22 July 2011; accepted 14 September 2011; published online 3 October 2011)

RF-sputtered TiO_x layers were thermally treated and the associated thin-film transistor properties were studied. X-ray diffraction and x-ray absorption spectroscopy analyses indicate that as-grown amorphous TiO_x films crystallize to anatase at temperatures above 450 °C in air. Thin-film transistors incorporating anatase active layers exhibit n-type behavior, with field effect mobility values near 0.11 cm^2/Vs when annealed at 550 °C. Such a phenomenon is suggested to originate from the ordering of Ti 3d orbitals upon crystallization, and the mobility enhancement at higher annealing temperatures may be attributed to the reduced grain boundary scattering of carriers by virtue of enlarged average grain size. © *2011 American Institute of Physics*. [doi:10.1063/1.3646105]

Thin-film transistors (TFTs) incorporating oxide semiconductors such as indium gallium zinc oxide (In-Ga-Zn-O)[1] have been subject of intensive research during the past several years for large area display applications. While the most common materials involve compounds based on indium and zinc such as In-Ga-Zn-O, In-Zn-O (Ref. 2) or Zn-Sn-O,[3] several research groups have recently suggested titanium oxide (TiO_x) as a cost-effective n-type semiconductor.[4,5] Deposition methods such as metal-organic chemical vapor deposition (MOCVD),[6] atomic layer deposition (ALD),[7] spray pyrolysis,[8] and magnetron sputtering[9] were employed to grow TiO_x active layers, which were implemented into working TFT devices.

In the above studies, titanium oxide was reported to exist in the amorphous state[6,7,9] or in one of its crystalline polymorphs, namely rutile[10] or anatase.[8] It was shown that TiO_x exhibits n-type transistor characteristics regardless of the microstructure, and such a behavior is generally attributed to the generation of free electrons originating from an oxygen deficient stoichiometry.[11,12] However, not much information is available on the conduction mechanism involving the electronic orbital structure of TiO_x. It is well known that the conduction band of TiO_x consists of overlapping Ti 3d orbitals,[10,13] yet detailed investigations on the ordering of the 3d orbitals in the material bulk and their effects on electrical conduction have not been performed up to date, especially concerning thin film transistors. In the present work, the microstructure and electronic orbital ordering of TiO_x layers upon heat treatment in air are examined, and the associated TFT behavior is analyzed.

Heavily doped p-type Si wafers with thermally grown SiO_2 were used as substrates onto which TiO_x films were deposited by radio frequency (RF) sputtering. An oxygen-deficient 3-in. TiO_x target (dark grey color) was used, and Ar gas was used to perform the sputtering. The final thickness of the TiO_x films was approximately 30 nm. The active islands were patterned using shadow masks, and subsequent thermal treatments were performed in air for 30 min at 450 °C and 550 °C. After annealing, 100 nm-thick indium tin oxide (ITO) source/drain electrodes were sputtered and patterned again using shadow masks. The resulting device width (W) and length (L) are 1000 μm and 150 μm, respectively.

Separate TiO_x films were prepared on identical substrates and subjected to the same heat treatments as for the TFT devices. X-ray photoelectron spectroscopy (XPS) and Rutherford backscattering spectroscopy (RBS) analyses of the TiO_x films yielded a Ti:O ratio of approximately 1:1.7, which reflects an oxygen deficient composition. The physical and electronic structures of the thermally treated TiO_x films were observed using x-ray diffraction (XRD) and x-ray absorption spectroscopy (XAS). The microstructure of TiO_x films was also observed by transmission electron microscopy (TEM).

Figure 1 shows the x-ray diffractograms (Figure 1(a)), the x-ray absorption spectrograms (Figure 1(b)), and plane-view bright-field TEM images (Figures 1(c)–1(e)) of the heat-treated TiO_x films. While the amorphous phase is preserved up to 300 °C, a phase transition to anatase occurs at 450 °C, as seen by the presence of the anatase (101) peak in the corresponding x-ray diffractogram. The crystallization is confirmed by TEM images, and once crystallized, the average grain size increases with annealing temperature, from approximately 200 nm at 450 °C to about 400 nm at 550 °C. An important feature in the XAS data is the splitting of the 3d orbital peaks as the material undergoes phase transition. More discussion is provided below in conjunction with electrical property analyses.

The TFT transfer curves were plotted by measuring the drain current (I_D) with respect to gate voltage (V_G) in air, maintaining a constant drain voltage (V_D) of 10 V (Figure 2(a)). As the TiO_x active layer crystallizes, semiconducting switching behavior is obtained (when annealed at 450 and 550 °C), whereas in the amorphous state, the device exhibits

a)Electronic mail: kbchung@dankook.ac.kr.
b)Electronic mail: jinseongpark@dankook.ac.kr.

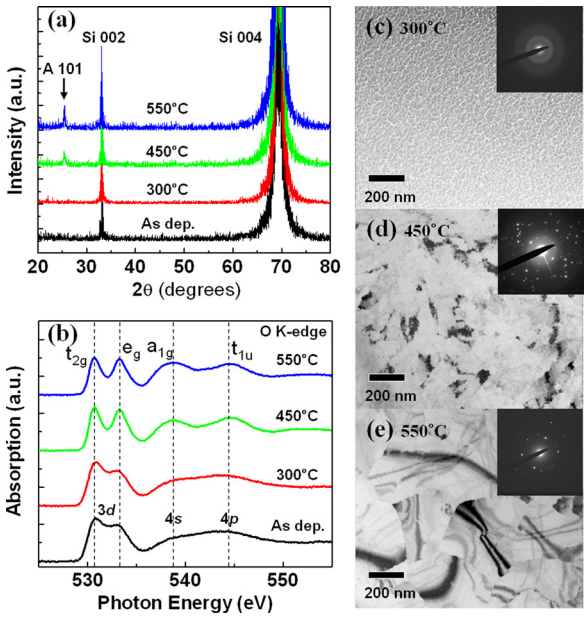

FIG. 1. (Color online) (a) X-ray diffractograms, (b) x-ray absorption spectra and bright field TEM images of TiO_x films annealed at (c) 300 °C, (d) 450 °C, and (e) 550 °C.

fully insulating characteristics. Typical pinch-off and hard saturation are observed in the output curves (I_D vs. V_D) of a working device (Figure 2(b)). Saturation field effect mobility values of 0.07 and 0.11 cm^2/Vs are obtained at annealing temperatures of 450 and 550 °C, respectively.

The crystallization itself does not account for the insulator to semiconductor transition, since many previous reports indicate semiconducting behavior in rutile,[10] anatase,[8] or amorphous[6,7,9] TiO_x TFT devices. It may then be assumed that the charge carrier density is of significant importance. Direct Hall measurements were attempted, and a carrier density of approximately $10^{13}\,cm^{-3}$ was obtained for the active layer annealed at 550 °C. For the as-grown film and the ones annealed at comparatively lower temperatures, the carrier density was below the instrument's detection limit so could not be measured. As an alternative way, the TiO_x bandgap and the relative position of the Fermi level with respect to the valence band maximum were analyzed by spectroscopic ellipsometry (SE) and XPS, as listed in Figure 3. The Fermi energy positions for the amorphous as-grown TiO_x and the one annealed at 450 °C are comparable, and rough calculations provide estimate carrier densities in the order of $10^{11}\,cm^{-3}$ for both. The effect of carrier density on the conducting behavior is, therefore, of minor importance in the present case.

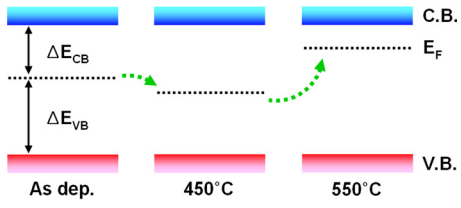

	E_g (eV)	ΔE_{VB} (eV)	ΔE_{CB} (eV)
As dep.	3.64	2.84	0.80
450°C	3.69	2.84	0.85
550°C	3.62	3.02	0.60

FIG. 3. (Color online) Schematic energy level diagrams reflecting the relative position of the Fermi level (E_F) with respect to the conduction band minimum (C.B.) and valence band maximum (V.B.) at different annealing temperatures. The corresponding values of the bandgap (E_g) and the relative energy difference between E_F and V.B. (ΔE_{VB}), and between E_F and C.B. (ΔE_{CB}) are indicated below the diagram.

The most compelling origin of the insulator to semiconductor transition may, thus, be attributed to the d orbital ordering, as observed in the XAS spectra. Normalized oxygen (O) K_1 edge spectra were analyzed in order to examine the electronic structure of the conduction band in TiO_x. The relative intensities of the XAS peaks reflect the qualitative changes in molecular orbital bonding symmetry.[14] The O K_1 edge spectra of TiO_x are directly related to the oxygen *p*-projected states of the conduction band, which consists of four unoccupied hybridized orbitals, t_{2g} (Ti 3d + O 2pπ), e_g (Ti 3d + O 2pσ) and two features corresponding to Ti 4sp + O 2p.[15] At annealing temperatures above 450 °C, considerable crystal-field splitting occurs in the 3d and 4sp orbitals, especially for the e_g states, which are related to the transition from TiO_2 to Ti_2O_3 with oxygen deficient stoichiometry.[16] This may be interpreted in such a way that molecular orbital ordering and the generation of oxygen vacant sites contribute to the enhanced electronic charge transport in TiO_x.

Once the semiconducting behavior is achieved, the field effect mobility enhancement by increasing the annealing temperature from 450 to 550 °C may be attributed to the increased average grain size. Scattering effects at grain

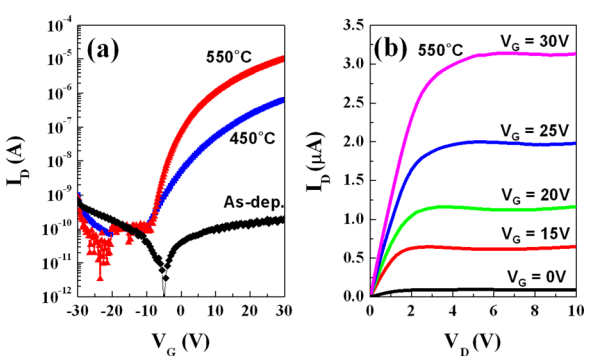

FIG. 2. (Color online) (a) Transfer curves of TiO_x TFT devices annealed at different temperatures and (b) output curves of the device with TiO_x annealed at 500 °C.

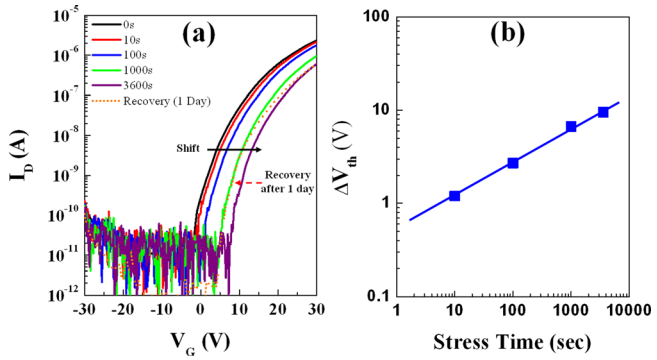

FIG. 4. (Color online) (a) Transfer curves shifting towards positive V_G values upon positive bias stress, with a slight recovery 1 day after the stress experiment. (b) The shift in threshold voltage (ΔV_{th}) upon bias stress.

boundaries is well known to impede charge transport across the active material bulk,[17] and once the density of such scattering centers is reduced, the mean free path of the charge carriers increases and so results in improved electrical conduction.

Besides the electrical performance, the behavior of the device upon bias stress was evaluated under positive bias stress, with a gate bias of 10 V while preserving a drain voltage of 10 V. Transfer curves were measured after 10, 100, 1000, and 3600 s of bias stress and then the stress was released. As illustrated in Figure 4(a), the transfer curves shift towards positive gate voltages with stress time, and after releasing the stress, a recovery in the negative direction is observed after 1 day. A linear relationship is obtained between log (V_{th}) and log (t) in Figure 4(b), which typically results from charge trapping at the semiconductor/gate insulator interface.[18] The slight recovery of the transfer characteristics without any external applied field or heat treatment is indicative of charge detrapping from shallow traps near the semiconductor/gate insulator interface, which necessitates relatively small energies. TiO_x TFT devices may, thus, be considered to behave in a similar fashion as other oxide semiconductor devices based on indium and zinc compounds.

To summarize, TiO_x films were sputter-deposited and annealed at different temperatures, with which TFT devices were fabricated. An electrically insulating amorphous structure persisted in the as-grown layer and at annealing temperatures up to 300 °C. Upon annealing at 450 °C and above, a structural phase transition occurred to anatase and semiconducting behavior was observed. The insulator to semiconductor transition is interpreted in terms of d orbital ordering, which provides highly conductive paths to charge carriers. Once the phase transition is achieved, higher annealing temperatures result in increased average grain size and carrier density, which is accompanied with field effect mobility values up to 0.11 cm^2/Vs upon thermal treatment at 550 °C.

Dr. Jin-Seong Park acknowledges financial support from the LCD division of Samsung Electronics, Inc., and the partial support from the Basic Science Research Program through the National Research Foundation (NRF), which is funded by the Korean Ministry of Education, Science and Technology (Grant Nos. 2011-0004433 and 2011-0004901).

[1]K. Nomura, H. Ohta, A. Takagi, T. Kamiya, M. Hirano, and H. Hosono, Nature **432**, 488 (2004).
[2]N. L. Dehuff, E. S. Kettenring, D. Hong, H. Q. Chiang, J. F. Wager, R. L. Hoffman, C.-H. Park, and D. A. Keszler, J. Appl. Phys. **97**, 064505 (2005).
[3]P. Görrn, M. Lehnhardt, T. Riedl, and W. Kowalsky, Appl. Phys. Lett. **91**, 193504 (2007).
[4]M. Katayama, S. Ikesaka, J. Kuwano, Y. Yamamoto, H. Koinuma, and Y. Matsumoto, Appl. Phys. Lett. **89**, 242103 (2006).
[5]J.-W. Park and S. Yoo, IEEE Electron Device Lett. **29**, 724 (2008).
[6]J.-W. Park, S.-W. Han, N. Jeon, J. Jang, and S. Yoo, IEEE Electron Device Lett. **29**, 1319 (2008).
[7]J.-W. Park, D. Lee, H. Kwon, and S. Yoo, IEEE Electron Device Lett. **30**, 739 (2009).
[8]P. H. Wöbkenberg, T. Ishwara, J. Nelson, D. D. C. Bradley, S. A. Haque, and T. Anthopoulos, Appl. Phys. Lett. **96**, 082116 (2010).
[9]K.-H. Choi and H.-K. Kim, Electrochem. Solid-State Lett. **14**, H314 (2011).
[10]M. Katayama, S. Ikesaka, J. Kuwano, Y. Yamamoto, H. Koinuma, and Y. Matsumoto, Appl. Phys. Lett. **89**, 242103 (2006).
[11]Y. Cheng, P. Xiong, L. Fields, J. P. Zheng, R. S. Yang, and Z. L. Wang, Appl. Phys. Lett. **89**, 093114 (2006).
[12]N. Huby, S. Ferrari, E. Guziewicz, M. Godlewski, and V. Osinniy, Appl. Phys. Lett. **92**, 023502 (2008).
[13]T. Hitosugi, H. Kamisaka, K. Yamashita, H. Nogawa, Y. Furubayashi, S. Nakao, N. Yamada, A. Chikamatsu, H. Kumigashira, M. Oshima, Y. Hirose, T. Shimada, and T. Hasegawa, Appl. Phys. Express **1**, 111203 (2008).
[14]K. B. Chung, J. P. Long, H. Seo, G. Lucovsky, and D. Nordlung, J. Appl. Phys. **106**, 074102 (2009).
[15]P. A. Cox, *Transition Metal Oxides* (Clarendon, Oxford, 1992).
[16]F. M. F. de Groot, M. Grioni, J. C. Fuggle, J. Ghijsen, G. A. Sawatsky, and H. Petersen, Phys. Rev. B **40**, 5715 (1989).
[17]Y. Furubayashi, N. Yamada, Y. Hirose, Y. Yamamoyo, and M. Otani, J. Appl. Phys. **101**, 093705 (2007).
[18]J. M. Lee, I.-T. Cho, J.-H. Lee, and H.-I. Kwon, Appl. Phys. Lett. **93**, 093504 (2008).